Published in final edited form as:
Neurobiol Aging. 2012 June ; 33(6): 1085–1095. doi:10.1016/j.neurobiolaging.2010.07.002.

Age-related increase of sI_{AHP} in prefrontal pyramidal cells of monkeys: relationship to cognition

Jennifer I. Luebke* and **Joseph M. Amatrudo**
Department of Anatomy and Neurobiology, Boston University School of Medicine, 72 East Concord St, Boston, MA 02118, USA

Abstract

Reduced excitability, due to an increase in the slow afterhyperpolarization (and its underlying current sI_{AHP}), occurs in CA1 pyramidal cells in aged cognitively-impaired, but not cognitively-unimpaired, rodents. We sought to determine whether similar age-related changes in the sI_{AHP} occur in pyramidal cells in the rhesus monkey dorsolateral prefrontal cortex (dlPFC). Whole-cell patch-clamp recordings were obtained from layer 3 (L3) and layer 5 (L5) pyramidal cells in dlPFC slices prepared from young (9.6 ± 0.7 years old) and aged (22.3 ± 0.7 years old) behaviorally characterized subjects. The amplitude of the sI_{AHP} was significantly greater in L3 (but not L5) cells from aged-impaired compared to both aged-unimpaired and young monkeys, which did not differ. Aged L3, but not L5, cells exhibited significantly increased action potential firing rates, but there was no relationship between sI_{AHP} and firing rate. Thus, in monkey dlPFC L3 cells, an increase in sI_{AHP} is associated with age-related cognitive decline; however, this increase is not associated with a reduction in excitability.

Keywords

Slice; Patch-clamp; Voltage-clamp; Potassium channels; Excitability

1. Introduction

Working memory, which is largely mediated by the dorsolateral prefrontal cortex (dlPFC), declines significantly during normal aging in a large proportion of rhesus monkeys (Bartus et al., 1979; Lai et al., 1995; Moore et al., 2003, 2006; Rapp, 1990; Steere and Arnsten, 1997). It is increasingly evident that there is not a single causative factor; rather, a multitude of changes in neuronal structure and function occur with normal aging which may together underlie cognitive decline (Dickstein et al., 2007). Relatively little is known about age effects on the functional electrophysiological properties of monkey neurons (but see Chang et al., 2005; Luebke et al., 2004; Luebke et al., 2010); by contrast, the effects of age on rodent hippocampal pyramidal cells have been extensively studied with *in vitro* slice recordings (for review: Barnes, 2003; Burke and Barnes, 2010; Thibault et al., 2007). These studies have shown that there is an age-related decrease in action potential firing rates of

*Correspondence to: Jennifer I. Luebke, Ph.D., M949, Department of Anatomy and Neurobiology, Boston University School of Medicine, 85 E. Newton St., Boston, MA 02118, USA; jluebke@bu.edu; voicemail: +1-617-638-4930; fax: 617-638-5954.

Disclosure: The authors have no actual or potential conflicts of interest.

CA1 pyramidal cells, with a concomitant increase in the amplitude of the calcium-dependent slow afterhyperpolarization (sAHP) responsible for spike frequency adaptation (Disterhoft et al., 1996; Landfield and Pitler, 1984; Power et al., 2002; for review: Faber and Sah, 2003; Thibault et al., 1998). Other studies have demonstrated that the age-related increase in magnitude of the sAHP is inversely related to performance on tasks mediated largely by the hippocampus, with aged-impaired subjects having significantly higher sAHP amplitudes than both aged-unimpaired and young subjects, which do not differ (Matthews et al., 2009; Moyer et al., 2000; Tombaugh et al., 2005).

These *in vitro* slice studies have led to a widely held view that age-related decline in hippocampal function can be attributed to reduced excitability and reduced synaptic plasticity of CA1 pyramidal neurons, secondary to increased calcium influx and amplitude of calcium-dependent sAHPs (for review: Faber and Sah, 2003; Foster, 2007; Thibault et al., 2007). While some *in vivo* single unit studies have reported an age-related decrease in CA1 pyramidal cell firing rates (Shen et al., 1997; Sava and Markus, 2008), a number of others have reported no change in firing rates of CA1 pyramidal cells (Barnes et al., 1983; Oler and Markus, 2000; Tanila et al., 1997) or of CA3 pyramidal cells (Oler and Markus, 2000; Tanila et al., 1997). Further, Wilson and coworkers (2005) reported no change in firing rates of CA1 pyramidal cells, but an increase in firing rates of CA3 pyramidal cells in the aged rat. Age-related increases in firing rates have also been reported for layer 3 pyramidal cells in *in vitro* slices of aged monkey dlPFC (Chang et al., 2005), and for visual cortical pyramidal cells in the aged monkey *in vivo* (Leventhal et al., 2003; Schmolesky et al., 2000; Zhang et al., 2008). In each case where increased excitability with age has been seen, it has been associated with decline in sensory or cognitive function (Chang et al., 2005; Leventhal et al., 2003; Schmolesky et al., 2000; Wilson et al., 2005; Zhang et al., 2008). While certainly functionally relevant, the cellular basis for age-related increases in neuronal excitability is unknown, but one plausible mechanism is a reduction in the amplitude of the current underlying the sAHP (the sI_{AHP}). This study was undertaken to determine whether there are age-related changes in the amplitude of the sI_{AHP} in monkey dlPFC pyramidal cells, and whether any such changes are related to alterations in excitability of these cells and/or to cognitive decline in the same monkeys.

2. Materials and methods

2.1. Experimental subjects

Rhesus monkeys obtained from the Yerkes National Primate Research Center were used in this study, which was part of an ongoing program of studies of normal aging. Monkeys were maintained at both the Yerkes National Primate Research Center and at the Boston University Laboratory Animal Science Center (LASC) in strict accordance with animal care guidelines as outlined in the NIH *Guide for the Care and Use of Laboratory Animals* and the U.S. Public Health Service Policy on Humane Care and Use of Laboratory Animals. All procedures were approved by the Institutional Animal Care and Use Committees of both the Yerkes National Primate Research Center and the Boston University LASC. Both institutions are fully accredited by the Association for Assessment and Accreditation of Laboratory Animal Care.

2.2. Assessment of cognitive function

Each monkey completed 6-9 months of testing on a variety of tasks designed to evaluate overall cognitive abilities. This testing consisted of the following: Delayed Non-Match to Sample (DNMS) basic (learning), DNMS performance at 2 and 10 minute delays, and the Delayed Recognition Span Task (DRST), with spatial and object modalities. Detailed descriptions on assessment and implementation of these tasks can be found in Herndon et al.

(1997). Significant impairment on individual behavioral tasks was defined as follows: greater than 210 errors for the DNMS basic task, less than 78% correct for the DNMS 2 and 10 minute delay tasks, and a span of less than 2.5 for the DRST spatial and object tasks (Herndon et al., 1997). The Cognitive Impairment Index (CII) is a composite score, calculated as an average of the standardized scores on the DNMS basic (10 second delay), DNMS 2 minute delay and the DRST spatial tasks using the guidance of a principal components analysis (Herndon et al., 1997). In the present study, monkeys were considered cognitively impaired if they received a CII *z*-score of more than 2.5 standard deviations greater than the mean for a large cohort of healthy, young monkeys.

2.3. Preparation of slices

Following completion of behavioral testing and structural MRI brain scans, monkeys were sacrificed. Monkeys were first tranquilized with ketamine (10 mg/ml), then deeply anesthetized with sodium pentobarbital (to effect, 15 mg/kg, I.V.). A thoracotomy was performed, and monkeys were killed by exsanguination while being perfused through the ascending aorta with ice-cold Krebs buffer (concentrations, in mM: 6.4 Na_2HPO_4, 1.4 Na_2PO_4, 137 NaCl, 2.7 KCl, 5 Glucose, 0.3 $CaCl_2$, 1 $MgCl_2$; pH = 7.4, chemicals from Sigma, St. Louis, MO). Prior to perfusion, a craniotomy was performed, and, immediately following perfusion, the dura was opened and a 10 mm^3 block of the dlPFC (area 46) removed. The tissue was quickly mounted and cut into 400 μm thick coronal slices with a vibrating microtome in ice-cold oxygenated Ringers solution (concentrations, in mM: 26 $NaHCO_3$, 124 NaCl, 2 KCl, 3 KH_2PO_4, 10 Glucose, 1.3 $MgCl_2$; pH = 7.4, chemicals from Sigma). Immediately after cutting, slices were placed in oxygenated, room temperature Ringers solution, where they were allowed to equilibrate for 1 hour. Following this equilibration period, a slice was placed in a submersion-type recording chamber (Harvard Apparatus, Holliston, MA), held down by a nylon mesh, and superfused with a continuous supply of oxygenated, room temperature Ringers solution (at a rate of 2-2.5 ml/min). Chambers were located on the stages of Nikon E600 infrared-differential interference contrast (IR-DIC) microscopes (MicroVideo Instruments, Avon, MA).

2.4. Whole-cell patch-clamp recordings

Pyramidal cells from either layer 3 or layer 5 of area 46 were visually identified under IR-DIC optics, and standard, tight-seal, whole-cell patch-clamp recordings were performed. Pipettes were pulled from borosilicate glass on a horizontal Flaming and Brown micropipette puller (Model P-87, Sutter Instruments, Novato, CA). The internal solution used in recording pipettes was as follows (concentrations, in mM): 100 potassium aspartate, 15 KCl, 3 $MgCl_2$, 5 EGTA, 10 Na-HEPES, 0.3 NaGTP, and 2 MgATP (pH = 7.4, chemicals from Fluka, NY), and electrodes had resistances of 3-6 MΩ in the external, Ringers solution. Experiments were performed with either List EPC-9 or EPC-10 patch-clamp amplifiers using either “Pulse” or “PatchMaster” acquisition software (HEKA Elektronik, Lambrecht, Germany). Access resistance was monitored throughout, and recordings were low-pass filtered at 10 kHz. To be included in the analyses, cells were required to exhibit repetitive action potential firing on depolarization, have a resting membrane potential negative to −55 mV, an action potential overshoot and stable access resistance.

2.5. Determination of intrinsic membrane properties and action potential firing rates

To determine passive membrane properties, including resting membrane potential (V_r) and input resistance (R_n), a series of 200 ms current pulses (14 steps, −160 to +100 pA) were applied from a membrane potential of −70 mV. V_r was measured as the potential present with 0 current input and R_n was determined as the slope of the best fit line through the plotted V-I data. To examine repetitive action potential firing properties, 2000 ms depolarizing current pulses (30, 180 and 280 pA) were applied, also from a membrane

potential of −70 mV. Data were analyzed using “Pulse-Fit” or “FitMaster” analysis software from HEKA Elektronik.

2.6. Characterization of the slow afterhyperpolarization current sI_{AHP}

The sI_{AHP} was evoked via a series of 200 ms depolarizing prepulse steps in voltage clamp (8 steps, −50 to +20 mV) from a holding potential of −55 mV (Fig. 1A). The amplitude of the sI_{AHP} was measured as the peak outward current ~20 ms after cessation of the step, during the return to holding voltage (Fig. 1A). The calcium-dependence of the current was demonstrated by its increasing amplitude following increasing amplitude (Fig. 1A) and duration (Fig. 1B) depolarizing prepulse voltage steps used to evoke calcium influx through high voltage-activated calcium channels. The voltage-independence of the current was demonstrated by a lack of change in the amplitude of the tail currents at the offset of increasing holding potential steps (Fig. 1C, arrow). Finally, the current was identified pharmacologically as being primarily comprised of the sI_{AHP} as it was largely blocked by the noradrenergic β-receptor agonist isoproterenol (Fig. 1D), but not significantly reduced by apamin (not shown).

2.7. Statistical analyses

Both behavioral and electrophysiological data were analyzed for statistical significance using a two-tailed Student’s *t*-test. To investigate relationships, linear (Pearson’s Product-Moment correlations) and quadratic regression analyses were performed. For statistical analyses, significance was defined as $p < 0.05$. Monkeys within the aged cohort were grouped into aged-impaired (AI) and aged-unimpaired (AU) groups based on their CII *z*-score. In addition, for each behavioral task, aged monkeys were grouped into AI or AU groups based on their performance on the specific task (with the exception of the DNMS 10 minute delay on which all aged animals were impaired). All data are reported as ± the standard error of the mean.

3. Results

3.1. Most but not all aged monkeys were cognitively impaired

A total of 12 young (6.0 – 12 years old) and 16 aged (17.6 – 27.0 years old) rhesus monkeys were used in the present study. Table 1 provides information on the monkeys used for layer 3 cell recordings and Table 2 provides the same information for monkeys used for layer 5 cell recordings. In 4 of the young and 5 of the aged monkeys, both layer 3 and layer 5 cells were examined and thus there is overlap in the monkeys listed in Tables 1 and 2. Each monkey successfully completed testing on the DNMS-basic, −2 minute and −10 minute delay tasks and the DRST-spatial and -object tasks (Tables 1 and 2). As a group, the aged monkeys used for layer 3 recordings were significantly cognitively impaired, as demonstrated by the mean CII *z*-score of 5.0 ± 1.2 compared to 0.7 ± 0.3 in the young group ($p < 0.005$). In the young layer 3 cohort, the CII *z*-score ranged from −0.03 to 2.3, with none considered to be impaired overall, while in the aged group the range was 0.55 to 11.9, with 8 of the 12 monkeys classified as significantly impaired and 4 as unimpaired (Table 1). Performance on every task was significantly worse in the aged group of monkeys compared to young (Table 1). Monkeys used for layer 5 recordings demonstrated a similar pattern of age-related cognitive impairment (Table 2).

3.2. Population of cells examined

For layer 3 pyramidal cell analyses, recordings were obtained from a total of 48 cells in slices prepared from 8 young monkeys and 82 cells from 12 aged monkeys, and for layer 5 analyses recordings were obtained from 38 cells from 8 young monkeys and 33 cells from 9

aged monkeys (Tables 1 and 2). Passive membrane properties (resting membrane potential and input resistance), action potential firing rates evoked by depolarizing current steps and slow afterhyperpolarization current (sI_{AHP}) properties were assessed for all layer 3 and layer 5 pyramidal cells (Table 3).

3.3. Passive membrane properties and action potential firing rates

Neither the resting membrane potential (V_r) nor the input resistance (R_n) were changed with age in layer 3 or layer 5 pyramidal cells (Table 3). Pyramidal cells responded to depolarizing current steps with trains of regular spiking action potentials that exhibited little spike frequency adaptation. Layer 3 pyramidal cells from aged monkeys fired action potentials at significantly higher rates than did those from young subjects at the +180 and +280 pA current steps ($p < 0.004$ and 0.03, respectively; Table 3). Cells in layer 5, however, did not display an age-related change in action potential firing rate (Table 3**).** These data are consistent with those previously published by our group (Chang et al., 2005;Luebke and Chang, 2007).

3.4. sI_{AHP} amplitude is significantly increased with age in layer 3 but not layer 5 cells

Increasing depolarizing voltage steps led to increased sI_{AHP} amplitude in all cells (Figs. 2A, C; 3A, C). At the voltage steps which activated the highest amplitude current (+10 and +20 mV) a significantly greater amplitude sI_{AHP} was seen in layer 3 cells from aged compared to young monkeys ($p < 0.05$; Table 3). This contrasts with layer 5 cells, which demonstrated no significant age-related change in sI_{AHP} amplitude (Table 3). When the mean maximal sI_{AHP} amplitudes of layer 3 cells from each monkey were plotted vs. age and a linear regression performed, a significant linear relationship was seen- with increasing amplitude sI_{AHP} associated with increased age ($p < 0.05$, r = 0.494, df = 18; Fig. 2B, left). Interestingly, these data were also well-fit by a quadratic function ($p < 0.01$, r = 0.850, df = 18; Fig. 2B, left, dashed line). The mean sI_{AHP} amplitude of layer 3 cells from monkeys within only the aged cohort also correlated with age ($p < 0.01$, r = 0.780, df = 10; Fig. 2B, right), demonstrating that the mean maximal sI_{AHP} amplitude increases progressively with advancing age. These relationships were not observed for sI_{AHP} amplitude in layer 5 cells vs. age (Fig. 3B).

The maximal amplitude of the sI_{AHP} was significantly greater in layer 3 cells from aged-impaired (AI) compared to aged-unimpaired (AU) and young monkeys (AI vs. AU: $p < 0.001$; AI vs. young: $p < 0.001$; AU vs. young: not significant; Figs. 2C, 4C). This was not the case for layer 5 pyramidal cells, where there was no significant difference in maximal sI_{AHP} amplitude between cells from AI, AU and young monkeys (Fig. 3C, 4D). Interestingly, when sI_{AHP} amplitude was plotted versus firing rate evoked by a strong depolarizing current step in the same cells, there was no significant relationship between the two variables in either layer 3 (r = 0.01, df = 125; Fig. 2D) or layer 5 cells (r = 0.085, df = 72; Fig. 3D).

3.5. The amplitude of the sI_{AHP} in layer 3 (but not layer 5) cells is significantly related to cognitive performance

The relationship between the amplitude of the sI_{AHP} and overall cognitive impairment was assessed by plotting the mean maximal amplitude of the current for all layer 3 or all layer 5 cells from a given monkey vs. that monkey's CII *z*-score (Figs. 4A, B). A linear regression was performed, and a significant relationship was found between mean sI_{AHP} amplitude in layer 3 cells and CII *z*-score ($p < 0.01$, r = 0.638, df = 18; Fig. 4A, top), but not between sI_{AHP} amplitude in layer 5 cells and CII *z*-score (Fig. 4B, top). The mean sI_{AHP} amplitude of layer 3 (but not layer 5) cells from monkeys within the aged cohort only also correlated with increased CII *z*-score ($p < 0.05$, r = 0.650, df = 10; Figs. 4A, B, bottom), demonstrating that mean maximal sI_{AHP} amplitude increases with increasing overall cognitive impairment

within the aged group. The mean amplitude of the sI_{AHP} was significantly greater in layer 3 cells from AI than from AU and young monkeys with mean maximal amplitudes of 172 ± 13 pA vs. 96 ± 12 pA and 108 ± 11 pA respectively ($p < 0.001$; Fig. 4C), but there was no difference in the mean amplitude of the current in layer 5 cells from the 3 groups (Fig. 4D).

The relationship between the maximal amplitude of the sI_{AHP} in layer 3 cells and impairment on each behavioral task was assessed by plotting the mean amplitude of the current for a given monkey vs. that monkey's performance on the task. No relationship between layer 5 sI_{AHP} amplitude and any behavioral task was found (CII: Fig. 4B; other tasks not shown). Performance on the DNMS basic task was significantly negatively correlated with the mean amplitude of the sI_{AHP} in layer 3 cells, both in all monkeys ($p < 0.01$, r = 0.661, df = 18; Fig. 5A, top) and within the aged cohort only ($p < 0.02$, r = 0.669, df = 10; Fig. 5A, bottom). By contrast, there was no significant linear relationship between the mean amplitude of the sI_{AHP} in layer 3 cells and performance on the DNMS 2 minute or 10 minute delay tasks (Fig. 5B, C). The mean amplitude of the sI_{AHP} in layer 3 cells from aged monkeys that were impaired on each individual task was compared to the amplitude in cells from those monkeys that were unimpaired on the task. The mean amplitude of the sI_{AHP} was significantly greater in layer 3 cells from aged animals that were impaired on the DNMS basic task compared to those that were from AU or from young monkeys ($p, < 0.001$; Fig. 5D). The mean amplitude of the sI_{AHP} was also significantly greater in layer 3 cells from aged animals that were impaired on the DNMS 2 minute delay task compared to young monkeys ($p, < 0.01$; Fig. 5E), however these cells did not differ from those from aged monkeys that were unimpaired on this task. All aged animals were impaired on the DNMS 10 minute delay task (thus, no AU data are presented in Fig. 5F) and a significant difference in the amplitude of the sI_{AHP} between young and aged monkeys was seen ($p < 0.05$).

There was a trend toward a significant relationship between increased mean amplitude of the sI_{AHP} in layer 3 cells and poorer performance on the DRST spatial task within the aged group ($p < 0.1$, r = 0.528, df = 10; Fig. 6A, bottom), but not within the overall cohort (Fig. 6A, top). Finally, there was no significant relationship between the mean amplitude of the sI_{AHP} in layer 3 cells and performance on the DRST object task (Fig. 6B). The mean amplitude of the sI_{AHP} was significantly greater in layer 3 cells from animals that were impaired on the DRST spatial tasks compared to AU or to young monkeys ($p < 0.01$; Fig. 6C), but only between AI and young on the DRST object task ($p < 0.02$; Fig. 6D).

Given that both CII and sI_{AHP} significantly increase with age, a partial correlation analysis was performed to determine if cognitive impairment *per se* is impacted by the increase in sI_{AHP}, or if the increase is simply an unrelated consequence of the aging process. Partial correlation analyses allow for the examining of one variable while controlling for variance in another, in this case controlling for age while examining the relationship between sI_{AHP} and CII. The *p*-value approached but did not quite meet statistical significance ($p = 0.059$). It seems likely that this is due to the variance in this relatively small sample. Hence it is suggestive of an overall non-zero association (i.e. a relationship of sI_{AHP} to CII, when age is controlled for) in the general population of monkeys.

4. Discussion

4.1. Age-related increase in the amplitude of the sI_{AHP} in layer 3 pyramidal cells

One of the most consistent findings in the aging literature is of a significant increase in the amplitude of the sAHP and/or its underlying current - the sI_{AHP} - in aged rodent hippocampal CA1 pyramidal cells (for review: Faber and Sah, 2003; Foster, 2007; Thibault et al., 2007). Here, we demonstrate that layer 3 pyramidal cells in *in vitro* slices of the primate dlPFC exhibit a similar age-related increase in sI_{AHP} amplitude. Thus, by contrast to

neuronal excitability, which has been reported to decrease, increase or remain the same with age depending on brain area and species, the sI_{AHP} amplitude has consistently been demonstrated to increase with age across brain areas and species. However, it should be noted that this phenomenon is not ubiquitous, given that the amplitude of the sI_{AHP} does not change with age in layer 5 pyramidal cells from the same monkeys. The observation of an age-related increase in sI_{AHP} amplitude in layer 3 but not layer 5 cells is of interest given the different roles of cells in the two cortical laminae; cortico-cortical layer 3 cells are thought to play a key role in cognitive function and to be especially vulnerable during aging, while primarily subcortically projecting layer 5 cells play a lesser role in cognitive function and may be relatively spared during aging (Morrison and Hof, 2002, 2007).

The present study did not directly address the mechanism of the age-related increase in sI_{AHP}. Perhaps the most straightforward explanation would be an age-related increase in the somatic membrane surface area, and thus in the total number of channels underlying the sI_{AHP}. However, layer 3 pyramidal cell soma size does not change with age (Peters, personal communication), and input resistance was the same in young and aged cells in the present study, arguing against this idea. Studies in the rodent hippocampus have clearly demonstrated that age-related changes in calcium homeostasis can directly impact the amplitude of this calcium-dependent current (Kumar and Foster, 2002; Norris et al., 1998; for review: Faber and Sah, 2003; Foster, 2007; Thibault et al., 2007). There is increased calcium influx in CA1 pyramidal cells with aging (Moyer et al., 1992; Power et al., 2002) due to an increase in density of high voltage-activated L-type calcium channels (Thibault and Landfield, 1996). There is also evidence for changes in ryanodine sensitive calcium-dependent calcium release with age, although consensus on this is lacking (Clodfelter, 2002; Gant et al., 2006; Kumar and Foster, 2004; for review: Foster, 2007; Thibault et al., 2007). In addition to being influenced by intracellular calcium levels, the sI_{AHP} is modulated by norepinephrine and acetylcholine, which reduce the sI_{AHP} open channel probability and thus its amplitude (Sah and Isaacson, 1995). Moore and coworkers (2005) reported significant reductions in noradrenergic markers, and Vannucchi and Goldman-Rakic (1991) reported a decreased affinity of M1 receptors for the muscarinic agonist carbachol in the dlPFC of aged monkeys. An age-related decline in these sI_{AHP} inhibitors could result in a disinhibition of the current and an increase in its amplitude. Further studies are required to determine which, if any, of these mechanisms underlie the significant increase in amplitude of the sI_{AHP} in the aged primate dlPFC.

4.2. Functional electrophysiological implications: firing rates of layer 3 pyramidal cells are not associated with sI_{AHP} amplitude

Changes in neuronal excitability and synaptic plasticity are frequently proposed to underlie cognitive decline during normal aging (for review: Barnes, 2003; Burke and Barnes, 2006; 2010; Faber and Sah, 2003; Foster, 2007; Thibault et al., 2007). Both excitability and synaptic plasticity can be strongly modulated by the sI_{AHP}, which acts by increasing spike frequency adaptation in the first case, and by shunting dendritic synaptic currents in the second (for review: Faber and Sah, 2003). Many previous *in vitro* slice studies have suggested that reduced excitability of CA1 pyramidal cells plays an important role in age-related impairment in hippocampal function in rodents. It is worth noting, however, that while some *in vivo* recording studies report a reduction in the firing rates of CA1 pyramidal cells with age (Shen et al., 1997; Sava and Markus, 2008), a number of others report that the firing rates of these cells are unaltered with age (Barnes et al., 1983; Oler and Markus, 2000; Tanila et al., 1997; Wilson et al., 2005). Furthermore, a number of studies have shown increased excitability of aged neurons - with recordings of pyramidal cells in *in vitro* slices of the monkey dlPFC (Chang et al., 2005), and with *in vivo* single unit recordings of CA3 pyramidal cells in rats (Wilson et al., 2005) and visual cortical pyramidal cells in the rhesus

monkey (Leventhal et al., 2003; Schmolesky et al., 2000; Zhang et al., 2008). Importantly, in these studies, increased firing rates were associated with age-related cognitive impairment in monkeys and rats (Chang et al., 2005; Wilson et al., 2005; respectively), and with degradation of visual stimulus selectivity in monkeys (Leventhal et al., 2003; Schmolesky et al., 2000; Zhang et al., 2008).

Age-related reduction in rodent CA1 pyramidal cell excitability is due to increased action potential firing frequency adaptation likely related to an age-related increase in sAHP amplitude (Disterhoft et al., 1996; Landfield and Pitler, 1984; Power et al., 2002; for review: Faber and Sah, 2003; Thibault et al., 1998). A key question addressed by the present study was whether the age-related increase in excitability of layer 3 dlPFC pyramidal cells in the monkey could be due to a decrease in the amplitude of the sI_{AHP}. The lack of a relationship between the amplitude of this current and action potential firing rates of layer 3 and layer 5 pyramidal cells argues strongly against this idea and suggests a dissociation between sI_{AHP} amplitude and action potential firing rates in these cells, which exhibit little spike frequency adaptation compared to hippocampal pyramidal cells. Our findings indicate that the age-related sI_{AHP} amplitude increase is not related to excitability changes in layer 3 pyramidal cells of the monkey dlPFC. Thus, the mechanism(s) underlying increased excitability of neurons with normal aging remains an open question.

4.3. Relationship of sI_{AHP} amplitude to performance on cognitive tasks

It is well known that significant cognitive impairment occurs with normal aging in many species, and that within any cohort of aged animals or humans there are successful-agers that are not impaired and unsuccessful-agers that are significantly impaired (Bartus et al., 1979; Herndon et al., 1997; Lai et al., 1995; Moore et al., 2003, 2005, 2006; Rapp, 1990; Steere and Arnsten, 1997). Thus, the demonstration that most, but not all, aged monkeys were significantly cognitively impaired in the present study is consistent with many previous studies. The findings in the aged rhesus monkey are consistent with findings in aged rodent CA1 pyramidal cells in that sI_{AHP} amplitude in layer 3 cells of aged monkey dlPFC correlated positively with increased cognitive impairment index (CII) *z*-score. Further, cells from monkeys that were impaired on the DNMS basic, DNMS 2 minute delay and DRST (both spatial and object) tasks exhibited significantly increased mean sI_{AHP} amplitude compared to those from young monkeys. The amplitude of the sI_{AHP} in cells from aged monkeys that were unimpaired on these tasks, by contrast, did not differ from young. The key question is - what discriminates between successful and unsuccessful aging individuals at a single neuron or network level? The inverse relationship between the amplitude of the sAHP in hippocampal pyramidal neurons recorded in *in vitro* slices and performance on both hippocampal-dependent and -independent conditioning tasks by subjects from which slices were prepared is well-established (Disterhoft et al., 1986, 1996; Matthews et al., 2009; Thompson et al., 1996; Tombaugh et al., 2005). This consistent finding has led to the hypothesis that reduction in sAHP amplitude may be a general mechanism by which neuronal excitability is increased during learning, and that an increase in sAHP amplitude leads to reduction in excitability and cognitive impairment in aging (e.g. Faber and Sah, 2003). The question arises as to whether similar mechanisms hold true in other brain areas, including the dlPFC of the aged monkey. Given the dissociation between sI_{AHP} amplitude and firing rate in dlPFC pyramidal cells shown in this study, a change in excitability due to a change in sI_{AHP} is not a plausible mechanism. The sI_{AHP} could also impact cognition by shunting incoming depolarizing synaptic potentials, thus raising the threshold for induction of synaptic plasticity (Sah and Bekkers, 1996; Thibault et al., 2001). This mechanism is consistent with the report of reduced synaptic excitation of these cells in aged monkey dlPFC slices (Luebke et al., 2004). Further work is needed to address the important question

of precisely how the increase in sI_{AHP} amplitude in layer 3 pyramidal cells relates to the decline in functions mediated by the dlPFC with normal aging in the primate.

Acknowledgments

Supported by NIH/NIA grants # P01 AG00001 and R01 AG025062 and NIH/NCRR #RR-00165. The authors are grateful to Dr. Douglas Rosene for performing perfusions of the monkeys and providing brain tissue from which recordings were obtained. We thank Johanna Crimins, Dr. Anne Rocher and Dr. Yu-Ming Chang for help with data acquisition and careful reading of the manuscript.

References

Barnes CA. Long-term potentiation and the ageing brain. Phil Trans Royal Soc - Series B: Biol Sci. 2003; 358(1432):765–772.

Barnes CA, McNaughton BL, O'Keefe J. Loss of place specificity in hippocampal complex spike cells of senescent rat. Neurobiol Aging. 1983; 4(2):113–119. [PubMed: 6633780]

Bartus JM, Dean RL, Fleming D. Aging in the rhesus monkey: effects on visual discrimination learning and reversal learning. J. Gerontol. 1979; 34:209–219. [PubMed: 108323]

Burke SN, Barnes CA. Neural plasticity in the ageing brain. Nat Rev Neurosci. 2006; 7(1):30–40. [PubMed: 16371948]

Burke SN, Barnes CA. Senescent synapses and hippocampal circuit dynamics. Trends Neurosci. 2010; 33(3):153–61. [PubMed: 20071039]

Chang Y, Rosene DL, Killiany RJ, Mangiamele LA, Luebke JL. Increased action potential firing rates of layer 2/3 pyramidal cells in the prefrontal cortex are significantly related to cognitive performance in aged monkeys. Cereb Cortex. 2005; 15:409–418. [PubMed: 15749985]

Clodfelter GV, Porter NM, Landfield PW, Thibault O. Sustained Ca^{2+}-induced Ca^{2+}-release underlies the post-glutamate lethal Ca^{2+} plateau in older cultured hippocampal neurons. Eur J Pharma. 2002; 447:189–200.

Dickstein DL, Kabaso D, Rocher AB, Luebke JI, Wearne SL, Hof PR. Changes in the structural complexity of the aged brain. Aging Cell. 2007; 6(3):275–284. [PubMed: 17465981]

Disterhoft JF, Coulter DA, Alkon DL. Conditioning-specific membrane changes of rabbit hippocampal neurons measured *in vitro*. Proc Natl Acad Sci. 1986; 83(8):2733–2737. [PubMed: 3458232]

Disterhoft JF, Thompson LT, Moyer JR, Mogul DJ. Calcium-dependent afterhyperpolarization and learning in young and aging hippocampus. Life Sci. 1996; 59:413–420. [PubMed: 8761329]

Faber ES, Sah P. Calcium-activated potassium channels: multiple contributions to neuronal function. Neuroscientist. 2003; 9(3):181–194. [PubMed: 15065814]

Foster TC. Calcium homeostasis and modulation of synaptic plasticity in the aged brain. Aging Cell. 2007; 6(3):319–325. [PubMed: 17517041]

Gant JC, Sama MM, Landfield PW, Thibault O. Early and simultaneous emergence of multiple hippocampal biomarkers of aging is mediated by Ca2+-induced Ca2+ release. J Neurosci. 2006; 26(13):3482–3490. [PubMed: 16571755]

Herndon JG, Moss MB, Rosene DL, Killiany RJ. Patterns of cognitive decline in aged rhesus monkeys. Behav Brain Res. 1997; 87:25–35. [PubMed: 9331471]

Lai ZC, Moss MB, Killiany RJ, Rosene DL, Herndon JG. Executive system dysfunction in the aged monkey: spatial and object reversal learning. Neurobiol Aging. 1995; 16(6):947–954. [PubMed: 8622786]

Landfield PW, Pitler TA. Prolonged Ca^{2+}-dependent afterhyperpolarizations in hippocampal neurons of aged rats. Science. 1984; 226(4678):1089–1092. [PubMed: 6494926]

Leventhal AG, Wang Y, Pu M, Zhou Y, Ma Y. GABA and its agonists improved visual cortical fuction in senescent monkeys. Science. 2003; 300(5620):812–815. [PubMed: 12730605]

Luebke JI, Barbas H, Peters A. Effects of normal aging on prefrontal area 46 in the rhesus monkey. Brain Res Rev. 2010; 62(2):212–232. [PubMed: 20005254]

Luebke JI, Chang Y. Effects of aging on the electrophysiological properties of layer 5 pyramidal cells in the prefrontal cortex. Neuroscience. 2007; 150:556–562. [PubMed: 17981400]

Luebke JI, Chang Y, Moore TL, Rosene DL. Normal aging results in decreased synaptic excitation and increased synaptic inhibition of layer 2/3 pyramidal cells in the monkey prefrontal cortex. Neuroscience. 2004; 125:277–288. [PubMed: 15051166]

Kumar A, Foster TC. 17beta-estradiol benzoate decreases the AHP amplitude in CA1 pyramidal neurons. J Neurophysiol. 2002; 88(2):621–626. [PubMed: 12163515]

Kumar A, Foster TC. Enhanced long-term potentiation during aging is masked by processes involving intracellular calcium stores. J Neurophysiol. 2004; 91(6):2437–2444. [PubMed: 14762159]

Matthews EA, Linardakis JM, Disterhoft JF. The fast and slow afterhyperpolarizations are differentially modulated in hippocampal neurons by aging and learning. J Neurosci. 2009; 29(15): 4750–4755. [PubMed: 19369544]

Moore TL, Killiany RJ, Herndon JG, Rosene DL, Moss MB. Impairment in abstraction and set shifting in aged rhesus monkeys. Neurobiol Aging. 2003; 24:125–134. [PubMed: 12493558]

Moore TL, Killiany RJ, Herndon JG, Rosene DL, Moss MB. Executive system dysfunction occurs as early as middle-age in the rhesus monkey. Neurobiol Aging. 2006; 27(10):1484–1493. [PubMed: 16183172]

Moore TL, Schettler SP, Killiany RJ, Herndon JG, Luebke JI, Moss MB, Rosene DL. Cognitive impairment in aged rhesus monkeys associated with monoamine receptors in the prefrontal cortex. Behav Brain Res. 2005; 160(2):208–221. [PubMed: 15863218]

Morrison JH, Hof PR. Selective vulnerability of corticocortical and hippocampal circuits in aging Alzheimer's disease. Prof Brain Res. 2002; 136:467–486.

Morrison JH, Hof PR. Life and death of neurons in the aging cerebral cortex. Int Rev Neurobiol. 2007; 81:41–57. [PubMed: 17433917]

Moyer JR, Thompson LT, Black JP, Disterhoft JF. Nimodipine increases excitability of rabbit CA1 pyramidal neurons in an age- and concentration-dependent manner. J Neurophysiol. 1992; 68(6): 2100–2109. [PubMed: 1491260]

Moyer JR, Power JM, Thompson LT, Disterhoft JF. Increased excitability of aged rabbit CA1 neurons after trace eyeblink conditioning. J Neurosci. 2000; 20(14):5476–5482. [PubMed: 10884331]

Norris CM, Halpain S, Foster TC. Reversal of age-related alterations in synaptic plasticity by blockade of L-type Ca2+ channels. J Neurosci. 1998; 18(9):3171–3179. [PubMed: 9547225]

Oler JA, Markus EJ. Age-related deficits in the ability to encode contextual change: a place cell analysis. Hippocampus. 2000; 10(3):338–350. [PubMed: 10902903]

Power JM, Wu WW, Sametsky E, Oh MM, Disterhoft JF. Age-related enhancement of the slow outward calcium-activated potassium current in hippocampal CA1 pyramidal neurons *in vitro*. J Neurosci. 2002; 22(16):7234–7243. [PubMed: 12177218]

Rapp PR. Visual discrimination and reversal learning in the aged monkey (*Macaca mulatta*). Behav Neurosci. 1990; 104(6):876–884. [PubMed: 2285486]

Sah P, Bekkers JM. Apical dendritic location of slow afterhyperpolarization current in hippocampal pyramidal neurons: implications for the integration of long-term potentiation. J Neurosci. 1996; 16(15):4537–4542. [PubMed: 8764642]

Sah P, Isaacson JS. Channels underlying the slow afterhyperpolarization in hippocampal pyramidal neurons: neurotransmitters modulate the open probability. Neuron. 1995; 15(2):435–441. [PubMed: 7646895]

Sava S, Markus EJ. Activation of the medial septum reverses age-related hippocampal encoding deficits: a place field analysis. J Neurosci. 2008; 28(8):1841–1853. [PubMed: 18287501]

Schmolesky MT, Wang Y, Pu M, Leventhal AG. Degradation of stimulus selectivity of visual cortical cells in senescent rhesus monkeys. Nature Neuroscience. 2000; 3(4):384–390.

Shen J, Barnes CA, McNaughton BL, Skaggs WE, Weaver KL. The effect of aging on experience-dependent plasticity of hippocampal place cells. J Neurosci. 1997; 17(17):6769–6782. [PubMed: 9254688]

Steere JC, Arnsten AF. The a-2A noradrenergic receptor agonist guanfacine improves visual object discrimination reversal performance in aged rhesus monkeys. Behav Neurosci. 1997; 111(5):883–891. [PubMed: 9383511]

Tanila H, Sipilä P, Shapiro M, Eichenbaum H. Brain aging: impaired coding of novel environmental cues. J Neurosci. 1997; 17(13):5167–5174. [PubMed: 9185554]

Thibault O, Gant JC, Landfield PW. Expansion of the calcium hypothesis of brain aging and Alzheimer's disease: minding the store. Aging Cell. 2007; 6:307–317. [PubMed: 17465978]

Thibault O, Hadley R, Landfield PW. Elevated postsynaptic $[Ca^{2+}]_I$ and L-type calcium channel activity in aged hippocampal neurons: relationship to impaired synaptic plasticity. J Neurosci. 2001; 21(24):9744–9756. [PubMed: 11739583]

Thibault O, Landfield PW. Increase in single L-type calcium channels in hippocampal neurons during aging. Science. 1996; 272(5264):1017–1020. [PubMed: 8638124]

Thibault O, Porter NM, Chen K-C, Blalock EM, Kaminker PG, Clodfelter GV, Brewer LD, Landfield PW. Calcium dysregulation in neuronal aging and Alzheimer's disease: history and new directions. Trends in Neurosci. 1998; 24:417–433.

Thompson LT, Moyer JR, Disterhoft JF. Transient changes in excitability of rabbit CA3 neurons with a time course appropriate to support memory consolidation. J Neurophysiol. 1996; 56(1):103–110.

Tombaugh GC, Rowe WB, Rose GM. The slow afterhyperpolarization in hippocampal CA1 neurons covaries with spatial learning ability in aged Fisher 344 rats. J Neurosci. 2005; 25(10):2609–2616. [PubMed: 15758171]

Vannucchi MG, Goldman-Rakic PS. Age-dependent decrease in the affinity of muscarinic M1 receptors in neocortex of rhesus monkeys. Proc Natl Acad Sci. 1991; 88(24):11475–11479. [PubMed: 1763062]

Wilson IA, Ikonen S, Gallagher M, Eichenbaum H, Tanila H. Age-associated alterations of hippocampal place cells are subregion specific. J Neurosci. 2005; 25(29):6877–6886. [PubMed: 16033897]

Zhang J, Wang X, Wang Y, Fu Y, Liang Z, Ma Y, Leventhal AG. Spatial and temporal sensitivity degradation of primary visual cortical cells in senescent rhesus monkeys. Eur J Neurosci. 2008; 28(1):201–7. [PubMed: 18616566]

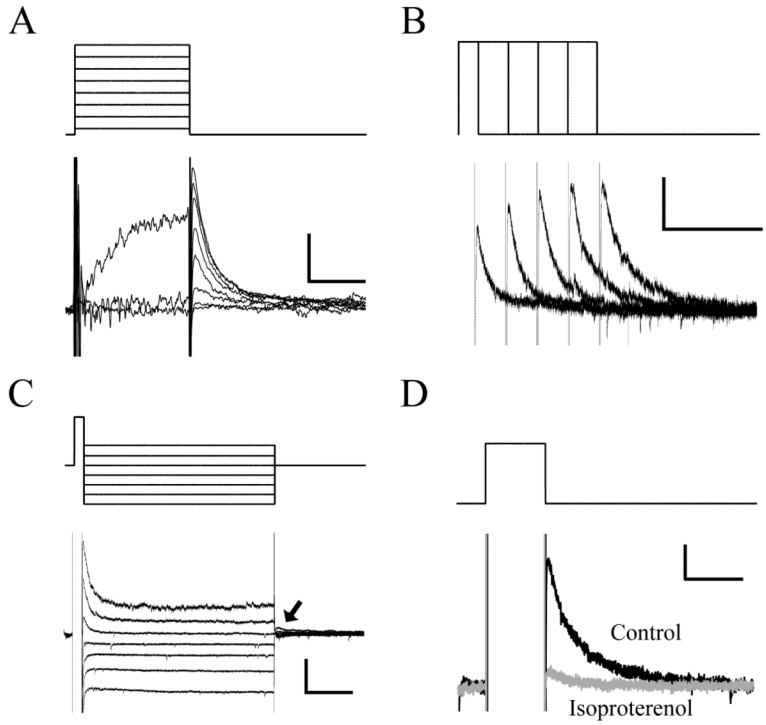

Figure 1.

Characterization of the sI_{AHP} in representative layer 3 pyramidal cells. A) Response to increasing amplitude depolarizing 200 ms voltage prepulses. B) Response of a representative layer 3 pyramidal cell to increasing duration depolarizing prepulses. C) Voltage-independence of the sI_{AHP} tail current demonstrated by a consistent step to −5 mV for 100 ms, followed by a voltage step to −95 to −35 mV. D) Near complete block of the sI_{AHP} by bath application of isoproterenol (10 μM). Scale bars: A= 35 mV, 100 pA/100 ms; B= 30 mV, 20 pA/1 s; C= 25 mV, 200 pA/500 ms; D= 30 mV, 100 pA/200 ms.

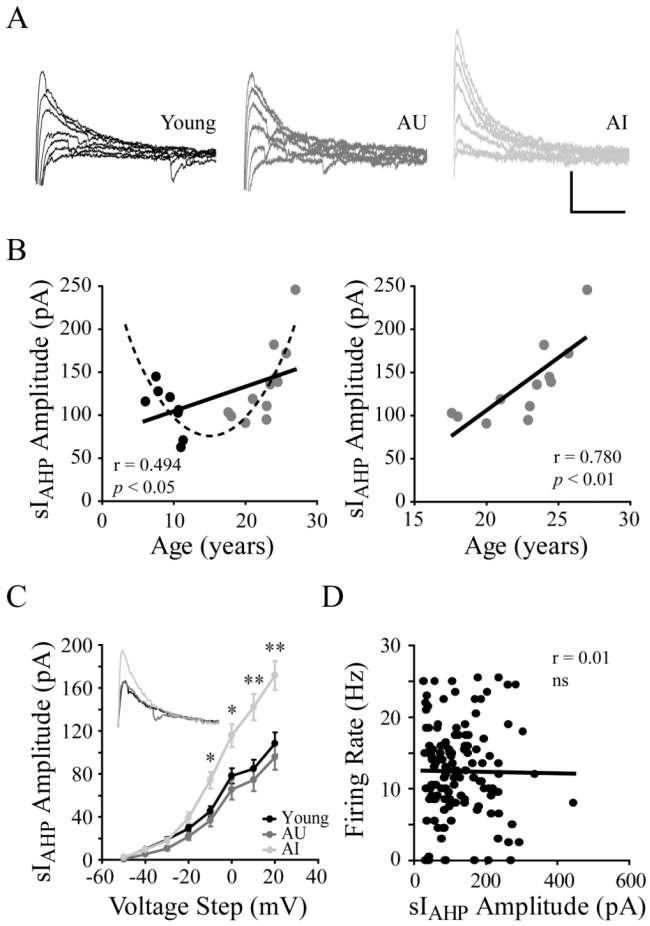

Figure 2.

The amplitude of the sI_{AHP} increases significantly with age in layer 3 pyramidal cells. A) sI_{AHP}s evoked by increasing depolarizing voltage steps in representative cells from young (left), aged-unimpaired (middle) and aged-impaired monkeys (right). B) Significant positive correlation between sI_{AHP} amplitude and age in all monkeys (left) and those within the aged cohort only (right). Additionally, a U-shaped quadratic equation was fit to the data obtained from all monkeys, and a significant relationship observed (dashed line). C) Line graph plotting mean sI_{AHP} amplitude as a function of voltage step for cells from young, aged-unimpaired and aged-impaired monkeys. Inset: superimposed traces of sI_{AHP}s evoked by +20 mV prepulses in cells from young, aged-unimpaired and aged-impaired monkeys. D) Mean sI_{AHP} amplitude vs. firing rate evoked by a +180 pA 2 s current step. Linear regression line demonstrates no significant relationship between sI_{AHP} amplitude and firing rate. Scale bars: 50 pA/100 ms. * $p < 0.01$; ** $p < 0.001$.

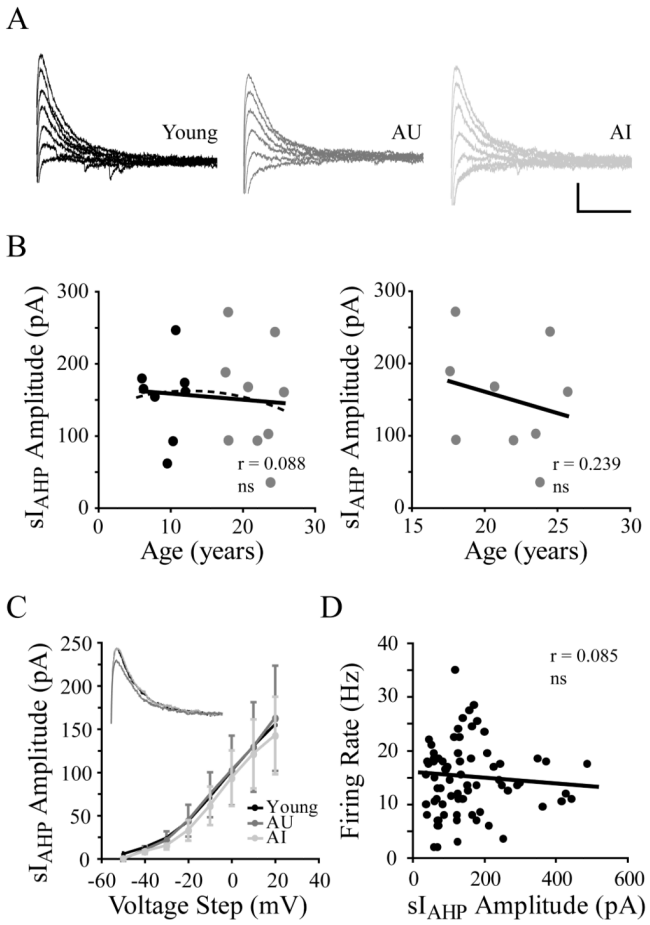

Figure 3.

The amplitude of the sI_{AHP} is unaltered with age in layer 5 pyramidal cells. A) sI_{AHP}s evoked by increasing depolarizing voltage steps in representative cells from young (left), aged-unimpaired (middle) and aged-impaired monkeys (right). B) No significant correlation between sI_{AHP} amplitude and age is seen in all monkeys (left) or in the aged cohort only (right). C) Line graph plotting mean sI_{AHP} amplitude as a function of voltage step for cells from young, aged-unimpaired and aged-impaired monkeys. Inset: superimposed traces of sI_{AHP}s evoked by +20 mV prepulses in cells from young, aged-unimpaired and aged-impaired monkeys. D) Mean sI_{AHP} amplitude vs. firing rate evoked by a +180 pA 2 s current step. Linear regression line demonstrates no significant relationship between sI_{AHP} amplitude and firing rate. Scale bars: 50 pA/100 ms.

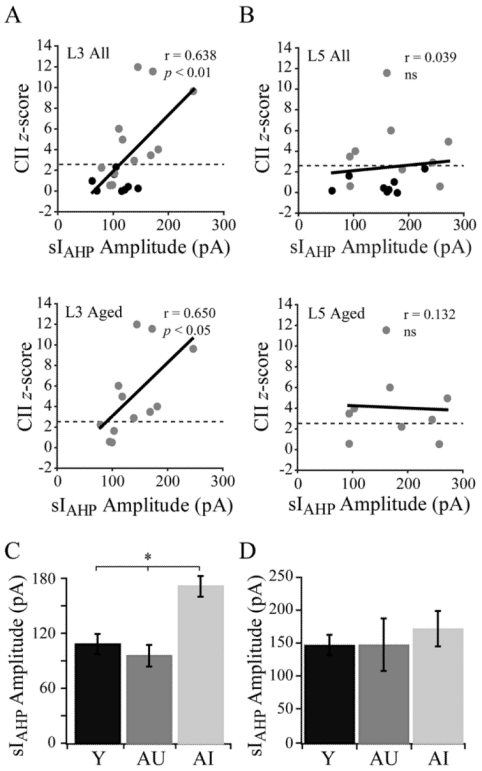

Figure 4.

Relationship of sI_{AHP} amplitude to overall CII *z*-score. A) Top, all subjects: mean sI_{AHP} amplitude in layer 3 pyramidal cells from a given monkey vs. the CII *z*-score for that monkey. Linear regression line demonstrates a significant positive correlation. Bottom, aged subjects only: mean sI_{AHP} amplitude for a given monkey vs. the CII *z*-score for that monkey. Linear regression line demonstrates a significant positive correlation. B) Top, all subjects: mean sI_{AHP} amplitude in layer 5 pyramidal cells for a given monkey vs. the CII *z*-score for that monkey. Linear regression line demonstrates no correlation. Bottom, aged subjects only: mean sI_{AHP} amplitude for a given monkey vs. the CII *z*-score for that monkey in the aged cohort of monkeys only. Linear regression line demonstrates no correlation. C) Bar graph giving mean sI_{AHP} amplitudes in layer 3 cells from young (n = 8), aged-unimpaired (n = 4) and aged-impaired monkeys (n = 8). D) Bar graph giving mean sI_{AHP} amplitudes in layer 5 cells from young (n = 8), aged-unimpaired (n = 4) and aged-impaired monkeys (n = 5). Dashed lines in A and B correspond to a *z*-score of 2.5, subjects with *z*-scores above this line are considered significantly impaired. * $p < 0.001$.

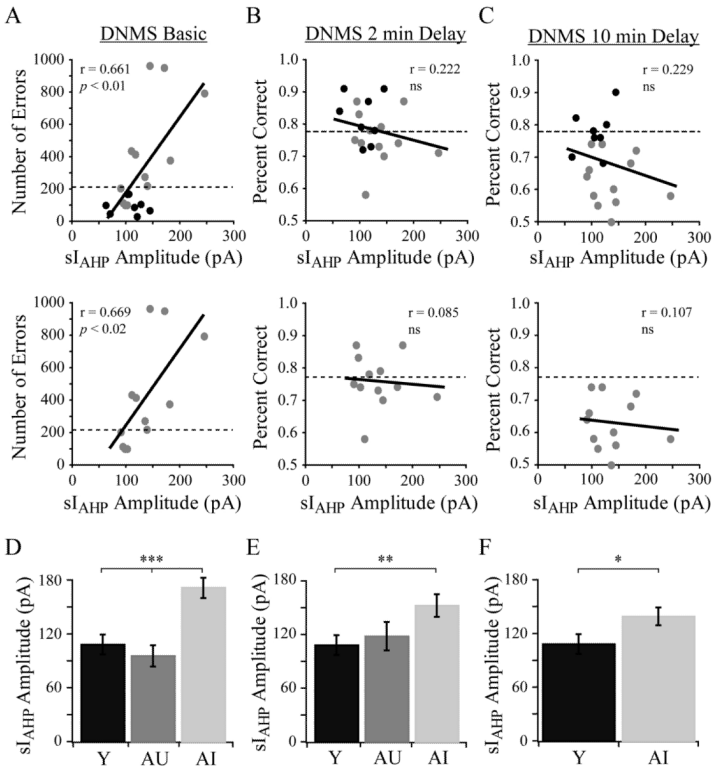

Figure 5.

Relationship of sI_{AHP} amplitude to performance on Delayed Non-Match to Sample behavioral tasks. Mean sI_{AHP} amplitude in layer 3 pyramidal cells from a given monkey vs. the monkey's performance on (A) DNMS basic, (B) DNMS 2 minute delay, and (C) DNMS 10 minute delay. Top: data from all monkeys, bottom: data from aged monkeys only. Bar graphs depicting mean sI_{AHP} amplitude in layer 3 pyramidal cells from young monkeys and aged monkeys that were either unimpaired or impaired on (D) DNMS basic, (E) DNMS 2 minute delay, or (F) DNMS 10 minute delay. Note that because all aged monkeys were impaired on the DNMS 10 minute delay task there is no aged-unimpaired group. Dashed lines in A, B and C correspond to the level above which (DNMS errors) or below which (DNMS 2 and 10 minute delay) a subject is considered significantly impaired. * $p < 0.05$; ** $p < 0.01$; *** $p < 0.001$.

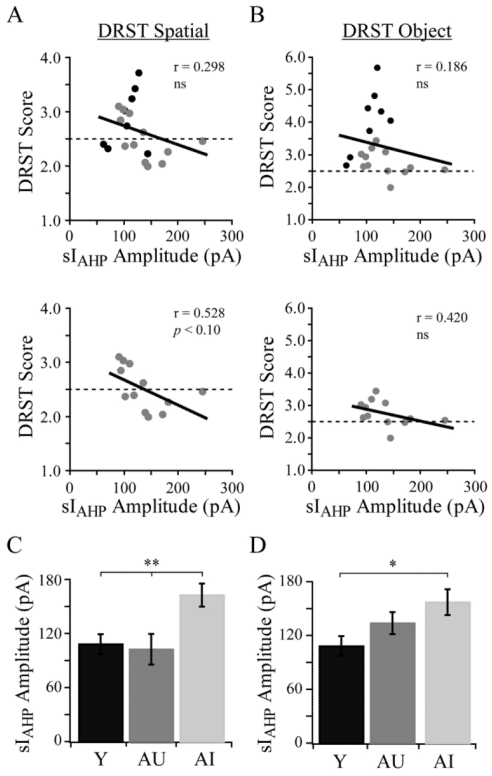

Figure 6.

Relationship of sI_{AHP} amplitude to performance on Delayed Recognition Span Tasks. Mean sI_{AHP} amplitude in layer 3 pyramidal cells from a given monkey vs. the monkey's performance on (A) DRST spatial and (B) DRST object behavioral tasks. Top: data from all monkeys, bottom: data from aged monkeys only. Bar graphs depicting mean sI_{AHP} amplitude in layer 3 pyramidal cells from young monkeys and aged monkeys that were either unimpaired or impaired on (C) DRST spatial or (D) DRST object tasks. Dashed lines in A and B correspond to the level below which a subject is considered significantly impaired. * $p < 0.02$; ** $p < 0.01$.

Table 1

Layer 3 Pyramidal Cells - Experimental Subjects

AM#	Sex	Age	CII	DNMSb Trials	DNMSb Errors	DNMS 2′ delay	DNMS 10′ delay	DRST Spatial	DRST Object
AM204	M	6	−0.03	446	85	0.87	0.76	3.23	4.80
AM230	M	7.5	0.27	220	66	0.91	0.90	2.22	4.04
AM198	F	7.8	0.41	439	104	0.78	0.80	3.71	4.32
AM255	F	9.5	0.12	100	29	0.73	0.68	3.42	5.66
AM199	F	10.6	1.61	732	168	0.79	0.78	3.01	4.42
AM214	F	10.7	2.30	759	168	0.72	0.76	2.73	3.73
AM254	F	11	0.97	329	99	0.84	0.70	2.40	2.66
AM197	F	11.3	−0.02	361	46	0.91	0.82	2.31	2.91
Mean		**9.3**	**0.70**	**423.3**	**95.6**	**0.82**	**0.78**	**2.88**	**4.07**
SEM		**0.74**	**0.32**	**86.6**	**19.4**	**0.03**	**0.03**	**0.21**	**0.37**
AM257	F	17.6	1.66	420	98	0.74	0.58	2.36	2.66
AM253	F	18	0.55	329	99	0.83	0.74	3.03	2.93
AM256	F	20	2.20	883	202	0.75	0.64	3.09	3.01
AM200	F	21	4.95	1283	414	0.78	0.74	2.38	3.43
AM236	M	22.9	0.58	360	112	0.87	0.66	2.84	2.62
AM242	M	23	6.01	1600	431	0.58	0.55	2.97	3.19
AM234	F	23.5	3.48	1253	271	0.73	0.50	2.62	3.07
AM235	F	24	4.00	1140	375	0.87	0.72	2.26	2.59
AM243	M	24.4	11.9	3626	962	0.70	0.56	1.99	1.98
AM189	M	24.5	2.90	728	217	0.79	0.60	2.06	2.49
AM220	F	25.7	11.5	2880	948	0.74	0.68	2.03	2.46
AM181	F	27	9.63	2253	792	0.71	0.58	2.45	2.53
Mean		**22.6**	**5.0**	**1396**	**410**	**0.76**	**0.63**	**2.51**	**2.75**
SEM		**0.88**	**1.22**	**314**	**96.3**	**0.02**	**0.02**	**0.12**	**0.12**
***p* <**		***0.0001***	***0.005***	***0.009***	***0.007***	***0.05***	***0.0003***	***0.05***	***0.0002***

CII= *z*-score; DNMS basic= total number of trials or errors; DNMS delay= % correct; DRST= average total span.

Table 2

Layer 5 Pyramidal Cells - Experimental Subjects

AM#	Sex	Age	CII	DNMSb Trials	DNMSb Errors	DNMS 2′ delay	DNMS 10′ delay	DRST Spatial	DRST Object
AM204	M	6	−0.03	446	85	0.87	0.76	3.23	4.80
AM205	M	6.2	0.08	231	54	0.80	0.88	3.24	6.32
AM198	F	7.8	0.41	439	104	0.78	0.80	3.71	4.32
AM255	F	9.5	0.12	100	29	0.73	0.68	3.42	5.66
AM202	F	10.3	0.45	360	99	0.86	0.64	2.90	4.15
AM214	F	10.7	2.30	759	168	0.72	0.76	2.73	3.73
AM194	F	11.9	2.26	764	156	0.74	0.66	2.43	2.99
AM195	F	12	−0.03	255	56	0.83	0.68	3.07	5.11
Mean		**9.3**	**0.70**	**419.3**	**93.9**	**0.79**	**0.73**	**3.09**	**4.64**
SEM		**0.9**	**0.38**	**90.7**	**18.5**	**0.02**	**0.03**	**0.15**	**0.40**
AM257	F	17.6	1.66	420	98	0.74	0.58	2.36	2.66
AM190	F	18	1.79	737	149	0.81	0.72	2.33	2.81
AM253	F	18	0.55	329	99	0.83	0.74	3.03	2.93
AM177	F	20.7	6.73	2060	518	0.69	0.42	2.37	2.79
AM208	M	22	1.09	300	74	0.75	0.60	2.66	3.66
AM234	F	23.5	3.48	1253	271	0.73	0.50	2.62	3.07
AM179	F	23.8	6.99	1559	505	0.69	0.67	1.84	1.82
AM189	M	24.5	2.90	728	217	0.79	0.60	2.06	2.49
AM220	F	25.7	11.5	2880	948	0.74	0.68	2.03	2.46
Mean		**21.5**	**4.1**	**1141**	**319.9**	**0.75**	**0.61**	**2.37**	**2.74**
SEM		**1.1**	**1.3**	**313**	**102.2**	**0.02**	**0.04**	**0.13**	**0.18**
***p* <**		***0.0001***	***0.03***	***0.05***	***0.05***	***0.16***	***0.02***	***0.002***	***0.001***

CII= *z*-score; DNMS basic= total number of trials or errors; DNMS delay= % correct; DRST= average total span.

Table 3

Electrophysiological Properties of dlPFC Pyramidal Cells

	YOUNG		AGED		
	Mean	**SEM**	**Mean**	**SEM**	***p* <**
LAYER 3					
Vr (mV)	−67.9	0.58	−67.1	0.49	*ns*
Rn (MΩ)	114.5	7.29	118.0	4.36	*ns*
Firing Rate (Hz)					
30 pA Step	0.99	0.43	1.42	0.32	*ns*
180 pA Step	10.3	0.95	13.6	0.62	*0.004*
280 pA Step	13.5	0.87	15.9	0.69	*0.03*
sI_{AHP} Amp (pA)					
−10 mV Step	45.1	5.07	57.3	5.27	*ns*
0 mV Step	78.3	7.64	95.7	7.84	*ns*
10 mV Step	84.7	9.09	112.4	8.90	*0.05*
20 mV Step	108.2	11.1	139.1	9.97	*0.05*
LAYER 5					
Vr (mV)	−66.3	0.83	−67.1	0.76	*ns*
Rn (MΩ)	150.0	7.21	148.8	7.49	*ns*
Firing Rate (Hz)					
30 pA Step	1.7	0.53	3.0	0.64	*ns*
180 pA Step	13.4	0.78	16.0	1.14	*ns*
280 pA Step	16.9	0.66	18.9	1.14	*ns*
sI_{AHP} Amp (pA)					
−10 mV Step	63.2	8.68	68.1	11.1	*ns*
0 mV Step	89.4	11.9	98.5	15.4	*ns*
10 mV Step	116.4	14.8	126.7	18.7	*ns*
20 mV Step	139.6	16.3	152.7	21.5	*ns*